

Characterization of (V₂O₅–WO₃) on TiO_x/Al₂O₃ Catalysts by ¹H-, ¹⁵N-, and ⁵¹V-Solid State NMR Spectroscopy

V. M. Mastikhin,* V. V. Terskikh,* O. B. Lapina,* S. V. Filimonova,*
M. Seidl,† and H. Knözinger†

*Boreskov Institute of Catalysis, Siberian Branch of Russian Academy of Sciences, 630090 Novosibirsk, Russia;
and †Institut für Physikalische Chemie, Universität München, Sophienstrasse 11, 80333 München, Germany

Received June 3, 1994; revised April 21, 1995

Vanadium and tungsten oxide supported on TiO_x/Al₂O₃ catalysts have been studied by solid state NMR spectroscopy. ¹H-MAS NMR spectra demonstrated that basic AlOH groups are involved in anchoring TiO_x and VO_x species. A certain percentage of the AlOH groups are located in positions, probably in the bulk of the alumina particles, where they remain inaccessible for interaction with titania, vanadia, or tungsten oxide. Titania modification of the Al₂O₃ surface leads to formation of bridging hydroxyls, namely Ti(OH)Ti and (or) Ti(OH)Al. Hydroxyl groups coordinated to Ti atoms are involved in anchoring vanadium and tungsten oxide species. VOH (and probably WOH) groups are formed when this ternary oxide phase is dispersed on the TiO_x/Al₂O₃ support. ⁵¹V-NMR spectra indicated that tungsten oxide participates in the formation of the structure of the mixed oxide surface complexes. ¹⁵N-NMR spectroscopy of adsorbed N₂O permitted the detection of strong Lewis acid sites on these multicomponent supported oxide catalysts. The acid strength of (V₂O₅–WO₃) on TiO_x/Al₂O₃ catalysts turned out to be comparable to that of the TiO_x/Al₂O₃ support material. © 1995 Academic Press, Inc.

INTRODUCTION

Supported vanadium oxide catalysts are important for several industrial processes, particularly selective oxidations (1) and selective catalytic reduction (SCR) of NO_x (1, 2). The preferred support for these applications is titania (anatase). This support, however, has a limited surface area and is relatively susceptible to sintering and phase transformation into rutile. Hence, composite supports containing titania dispersed on silica (3–12) and alumina (13) have received some attention in recent years. With alumina as a primary support, which is available as a washcoat on thermally and mechanically stable ceramic carriers, technologically advantageous catalyst supports may be obtained when titania can be grafted onto the alumina washcoat. The use of TiO₂/Al₂O₃ supports for supported vanadia catalysts seems to provide the additional advan-

tage in the SCR reaction that the catalyst fouling by ammonium hydrogen sulfate deposition produced from SO₂ in the feed is significantly reduced (14).

Practical SCR catalysts typically contain V₂O₅ together with WO₃ and/or MoO₃, one of the desirable functions of the WO₃ being the reduction of the activity of the catalysts for SO₂ oxidation (15). Catalysts containing exclusively WO₃ are active in SCR (2, 15), while the addition of V₂O₅ enhances their low temperature activity. The SCR reaction on mixed (V₂O₅–WO₃)/TiO₂ catalysts has been studied by Tuentner *et al.* (16). Chen and Yang (17) reported that the presence of WO₃ in titania-supported SCR catalysts increased their activity and their resistance toward poisoning by alkali metal oxides and arsenious oxide and reduces their activity for NH₃ and SO₂ oxidation. The same authors also suggested that Brønsted sites were the active sites for the SCR reaction and that the addition of WO₃ increased both the density of Brønsted sites and their acid strength.

Studies on WO₃ and (V₂O₅ + WO₃) supported on TiO₂/Al₂O₃ have not been reported to the best of our knowledge. Therefore, we present here a structural investigation of these materials using ¹H-, ¹⁵N-, and ⁵¹V-solid state NMR as the analytical technique. ⁵¹V-NMR provides unique information on the local environment of vanadium and is thus excellently suited for the structural characterization of vanadia-containing catalysts (18–23). Eckert and Wachs (19) showed that the nature of the support had a strong influence on the distribution of tetrahedrally and octahedrally coordinated VO_x species. Thus, TiO₂ (anatase) favoured six-coordinated species, while γ-Al₂O₃ had a higher tendency toward stabilizing four-coordinated vanadia species. ¹H-MAS NMR provides additional information on the density of hydroxyl groups and their Brønsted acid strength (22, 24), while ¹⁵N-NMR of adsorbed N₂O probe molecules permits the detection of Lewis acid sites (25). Thus, the combined application of these three nuclei for NMR studies permitted a structural characterization and an analysis of the acid properties of vanadium- and

tungsten-oxide containing catalysts supported on $\text{TiO}_2/\text{Al}_2\text{O}_3$.

EXPERIMENTAL

Sample Preparation

Alumina was prepared by calcination of $\text{Al}(\text{OH})_3$ at 700°C for 5 h. The resulting oxide was a mixture of mainly the η modification and some γ - Al_2O_3 according to X-ray diffraction analysis, and had a BET surface area of $130\text{ m}^2/\text{g}$.

For modification of this support material by TiCl_4 (Merck, Darmstadt, Germany), the grafting technique as applied by Fogar and Anderson (26) and by Wei *et al.* (13) was used. Dry N_2 gas was passed over the alumina in a glass reactor at 200°C for 1 h. Subsequently, the N_2 gas was saturated with TiCl_4 which was allowed to react with the alumina at 200°C for 2 h. The reactor was then flushed with dry N_2 for 1 h to remove excess TiCl_4 and the chemisorbed species were hydrolyzed by passing water-vapor-saturated N_2 over the sample at 200°C for 1 h, followed by calcination at 450°C for 5 h. A part of the resulting titania-modified material was treated a second time under identical conditions in order to obtain two supports containing different amounts of titania. The materials will be denoted AlTi1 and AlTi2 throughout this paper. They contained 3.7 and 8.8 wt% TiO_2 and had BET surface areas of 211 and $181\text{ m}^2/\text{g}$, respectively. The formation of anatase is indicated by X-ray diffraction in both samples, the relative amounts being higher for sample AlTi2 than for AlTi1, as expected.

Vanadium- and tungsten-oxide-containing catalysts were prepared by wet impregnation of the titania-modified alumina supports: V_2O_5 and WO_3 were dissolved in a mixture of 20 ml of 30% NH_3 and 80 ml distilled water and the solution was stirred with 12 g of the AlTi supports for 3 h. The water was then evaporated in a rotary evaporator, the resulting solid material was dried at 120°C for 15 h and calcined at 450°C for 5 h. Concentrations in the impregnation solution were chosen such that the final catalysts contained 3 wt% V_2O_5 and 10 wt% WO_3 . These materials will be denoted VWAlTi1 and VWAlTi2. Their BET surface areas were 184 and $166\text{ m}^2/\text{g}$, respectively.

^1H -MAS NMR Spectroscopy

^1H -MAS NMR spectra were measured on a Bruker CXP-300 NMR spectrometer (magnetic field 7.04 T, resonance frequency for ^1H nuclei 300.066 MHz). The frequency range was 50 kHz, the pulse width was 5 μs , and the recycle time 20 s. Usually 200 to 500 free induction decays were accumulated. The chemical shifts were measured relative to an external tetramethylsilane standard with an accuracy of ± 0.2 ppm. Prior to the

NMR measurement, the samples (0.1–0.3 g) were placed into 7 mm o.d., 12-mm-long glass sample tubes and evacuated (pressure 10^{-3} Pa) at temperatures of 300 or 500°C for 12–14 h, then treated in O_2 at 4×10^4 – 5×10^4 Pa for 1 h at the evacuation temperature, followed by evacuation at room temperature for 2 h to remove oxygen. After this treatment the sample tubes were sealed off and placed in the Andrew–Beams quartz rotor. The rotation frequency was about 3 kHz.

The exchange of OH groups on the oxide surfaces was performed by exposure to D_2O (saturated vapor pressure) at room temperature on samples which had been evacuated at 300 or 500°C . After contact with D_2O vapor for 1 h, the samples were evacuated at 300 and 500°C , respectively.

The content of OH groups in the samples was determined quantitatively by comparison of the ^1H -NMR signal intensity with that of a standard sample (SiO_2 evacuated at 300°C and containing 5×10^{19} protons).

Complex experimental spectra with overlapping lines were decomposed into Gaussian components (r.m.s. $\leq 10\%$). The chemical shift values of individual lines thus obtained were measured with an accuracy of ± 0.2 ppm. The error of intensities of individual lines was less than 10%.

^{15}N -NMR Spectroscopy

The ^{15}N -NMR spectra of adsorbed N_2O were recorded at 40.6 MHz using a Bruker MSL-400 spectrometer (magnetic field 9.39 T). Pulses of 10–12 μs duration with a repetition time of 2 s were used. The ^{15}N chemical shifts (δ) were measured relative to liquid nitromethane. The spectral range was 15–20 kHz and the number of the signal accumulations (NS) varied from 10^3 to 3×10^4 . All NMR measurements were carried out at room temperature.

Prior to NMR experiments, the catalysts were placed into special glass tubes (10 mm o.d., 35 mm length) and evacuated at 500°C to a pressure of 10^{-3} Pa for 12–14 h. After adsorption of N_2O at room temperature, the samples were sealed off. Vanadia-containing catalysts were subjected to an additional treatment in oxygen (4×10^4 – 5×10^4 Pa) at evacuation temperature for 1 h prior to N_2O adsorption. Amounts of the adsorbate (between 60 and 600 $\mu\text{mol/g}$) were measured volumetrically. N_2O enriched to 60% with the ^{15}N isotope was used.

^{51}V -NMR Spectroscopy

^{51}V -NMR spectra were measured using a Bruker MSL-400 spectrometer (magnetic field 9.39 T) at 105.2 MHz in a frequency range of 250 kHz. Pulses of 2 μs radio-frequency were used. The pulse repetition frequency was 5 Hz. Magic angle spinning was performed at a rotation frequency of 4–5 kHz. ^{51}V chemical shifts were measured with respect to an external VOCl_3 standard. Prior to the

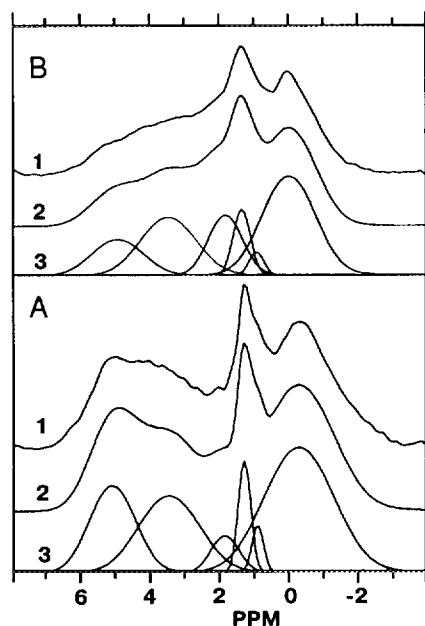


FIG. 1. ^1H -MAS NMR spectra of Al_2O_3 treated in vacuum (10^{-3} Pa) at 300°C (A) and 500°C (B) with their decomposition into Gaussian lines: (1) experimental spectrum; (2) best fitted spectrum; (3) decomposition of spectrum into Gaussian lines. The spectra of Al_2O_3 catalysts are measured at 300 MHz.

measurements, samples were placed in quartz ampoules (10 mm o.d., 40 mm length), heated in air at 500°C for 2 h, evacuated for 1 h (at 200 or 500°C) and heated in oxygen (4×10^{-4} – 5×10^{-4} Pa) for 1 h at the same temperature. Then, the samples were cooled to room temperature, evacuated, and sealed.

RESULTS AND DISCUSSION

1. ^1H -MAS NMR Spectra

1.1. Alumina. Figure 1 illustrates the ^1H -NMR spectra of Al_2O_3 after evacuation at 300°C (A) and 500°C (B). The decomposition of the spectra into Gaussian lines shows that at least six lines with chemical shifts from -0.3 to 5 ppm are superimposed in the spectra (Fig. 1). Their intensities decrease upon increasing the treatment temperature. This effect is more pronounced for the low field components (δ from 5 to 2 ppm, Fig. 1). The different lines in the ^1H spectra of Al_2O_3 indicate the presence on its surface of OH groups with different molecular environments around the protons, in accordance with the model of the Al_2O_3 surface proposed by Knözinger and Ratnasamy (27). According to this model, five main types of isolated OH groups with different electronic charges on the protons should be present on alumina surfaces. A structural analysis of the planes of Al_2O_3 shows that OH groups on the surface of γ - Al_2O_3 can coordinate to one, two, or three

Al^{3+} ions in octahedral coordination (type Ib, IIb, and III OH groups, respectively). In addition, OH groups can be coordinated to one tetrahedral Al^{3+} cation (type Ia OH group) and they can bridge a tetrahedral and an octahedral Al^{3+} cation (type IIa OH groups). This is also valid for other crystal modifications of Al_2O_3 (η , χ , θ , δ). The attribution of ^1H -NMR lines to these different types of OH groups in γ - and α - Al_2O_3 was reported earlier (28), where the peak at high field ($\delta \approx -0.3$ ppm) was ascribed to the most basic OH group (type Ib) and the unresolved peak at 2.5–3 ppm was proposed to belong to the more acidic OH groups. The ^1H -MAS NMR spectrum of the present alumina sample (mainly η - Al_2O_3 and some γ - Al_2O_3) is different from that for γ - Al_2O_3 . It has an increased intensity of the high-field peaks ($\delta \approx -0.3$ ppm) and a peak near 1.4 ppm; at the same time the poorly resolved low-field peaks at 3–5 ppm are shifted to lower field as compared with the 2.5–3 ppm for γ - Al_2O_3 reported earlier (28). This reflects the difference in the structure of the surface of γ - and η - Al_2O_3 . The latter has a less densely packed structure and is usually claimed to be more acidic than γ - Al_2O_3 (27). For γ - Al_2O_3 the (110) and (100) surface planes are predominant, while for η - Al_2O_3 the (110) plane most commonly represents the crystal surface (29).

The larger shift of the down-field peak to low-field for η - Al_2O_3 compared with γ - Al_2O_3 is most probably suggestive of hydrogen bonding between more closely spaced OH groups in η - Al_2O_3 . This effectively facilitates the dehydroxylation process. Indeed, the intensity of the low-field peak of η - Al_2O_3 decreases considerably after evacuation at 500°C (Fig. 1), while this peak predominates in the spectrum of γ - Al_2O_3 treated at the same conditions (see Ref. (22), Fig. 2). This means that dehydroxylation at 500°C almost completely removes the most acidic surface OH groups at 5 ppm of η - Al_2O_3 . It is also remarkable that a peak at $\delta = 1.4$ ppm, which was not normally observed in the spectra of γ - Al_2O_3 , manifests itself in the spectra of η - Al_2O_3 after its dehydroxylation at 300 and 500°C (Fig. 1). Usually, isolated water molecules which are not engaged in hydrogen bonds with each other produce a signal at about this value. Tentatively a peak at 1.4 ppm might be attributed to isolated water molecules located in closed pores from which they cannot be desorbed on evacuation at 300°C. However, even after evacuation of the sample at 500°C this line still remains in the spectrum. Most probably it consists of two overlapping lines, one belonging to water molecules in closed pores and the second one being caused by OH groups. This conclusion is also based on the H–D exchange results which show that a considerable amount of this signal remains after H–D exchange at both 300 and 500°C. Decomposition of the spectra indeed shows that a peak at 1.4 ppm could be represented as consisting of two closely spaced lines. One of them is supposed to belong to water in closed pores (Fig. 1).

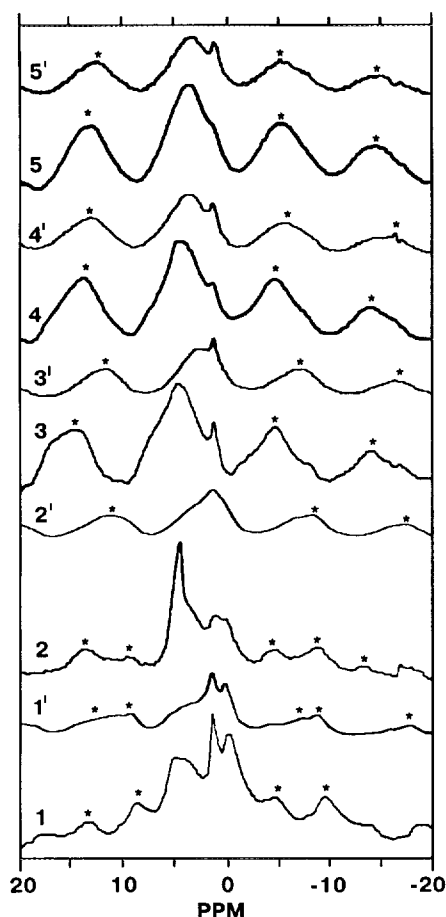


FIG. 2. ^1H -MAS NMR spectra of Al_2O_3 (1, 1') and of catalysts prepared by the grafting of Al_2O_3 with TiCl_4 : (2, 2') 3.7 wt% TiO_2 (AlTi1); (3, 3') 8.8 wt% TiO_2 (AlTi2). With supported V_2O_5 (3 wt%) and WO_3 (10 wt%): (4, 4') on AlTi1 (VWAITi1); (5, 5') on AlTi2 (VWAITi2). Before measurements samples were evacuated at 300°C (1–5) and 500°C (1'–5'). Asterisks indicate spinning side bands, which are symmetrically located relative to the central line. Spacing between the first side band and central line (in Hz) is equal to the sample rotation frequency.

1.2. Catalysts supported on Al_2O_3 . ^1H -MAS NMR spectra of catalysts supported on Al_2O_3 are presented in Figs. 2 and 3. The total concentrations of protons in the samples are summarized in Table 1. When 3.7 wt% TiO_2 is supported on Al_2O_3 the ^1H -MAS NMR spectrum (spectrum 2 in Fig. 2) is significantly different from that of pure Al_2O_3 . For this sample, AlTi1 evacuated at 300°C , a considerable decrease in intensity of the line of the most basic type Ib OH groups of alumina ($\delta = -0.3$ ppm) is observed. The intensity of the line at $\delta = 1.4$ ppm also decreases. This indicates the interaction of TiO_x species with the most basic OH groups of alumina. This conclusion is strongly supported by *in situ* DRIFT spectra (not shown) which clearly show the erosion of OH stretching bands typical for the basic alumina hydroxyl groups when TiO_x is deposited on the alumina surface.

The line of "acidic" OH groups can be seen as a shoulder of the line at $\delta = 4.8$ ppm which is attributed to water molecules that still cannot be evacuated at 300°C . The narrow width of the line at 4.8 ppm and the absence of side bands indicate relatively high mobility of the corresponding species. This suggests that TiO_x surface species possess a structure which includes H_2O in the Ti^{4+} coordination sphere. The signal from H_2O obscures the observation of new OH groups after evacuation at 300°C if the latter are formed by supporting TiO_x . However, after evacuation at 500°C the signal from H_2O disappears and a line at about 2–3 ppm develops in spectrum 2' of Fig. 2. The increase of the TiO_2 content results in a complete disappearance of the signal of basic OH groups (δ from -0.1 to -0.3 ppm), indicating a more complete interaction of the alumina surface with supported TiO_x species (spectra 3 and 3' in Fig. 2). The peak at $\delta = 1.4$ ppm still remains in the spectra. Simultaneously, an asymmetric line in the region 7 to 5 ppm, which is composed of two or more unresolved lines, manifests itself in spectrum 3 in Fig. 2. A line at about 7 ppm is typical for bridging Ti–OH–Ti groups, similar to those found on anatase (30). A narrow signal of molecular water does not remain in the spectrum of this sample. Therefore, the structure of surface TiO_x species must have changed as the TiO_2 content increases since surface species no longer contain strongly bonded H_2O molecules. They contain bridging Ti–OH–Ti and, probably, Ti–OH–Al groups, the latter groups presumably having values of chemical shifts close to those for Ti–OH–Ti. The total concentration of OH groups in the samples does not change considerably (Table 1), suggesting that along with the disappearance of basic Al–OH groups new OH groups coordinated to TiO_x species appear on the catalyst surface.

When supporting vanadium and tungsten oxide on AlTi,

TABLE 1
Total Content of OH Groups in Al_2O_3 and in Supported AlTi and VWAITi Catalysts

Sample	Pretreatment temperature ($^\circ\text{C}$)	OH groups (± 0.5) $\times 10^{20} \text{ g}^{-1}$
Al_2O_3		5.2
AlTi1		5.2
AlTi2	300	6.0
VWAITi		4.9
VWAITi2		6.0
Al_2O_3		3.5
AlTi1		3.2
AlTi2	500	2.0
VWAITi1		2.8
VWAITi2		3.1

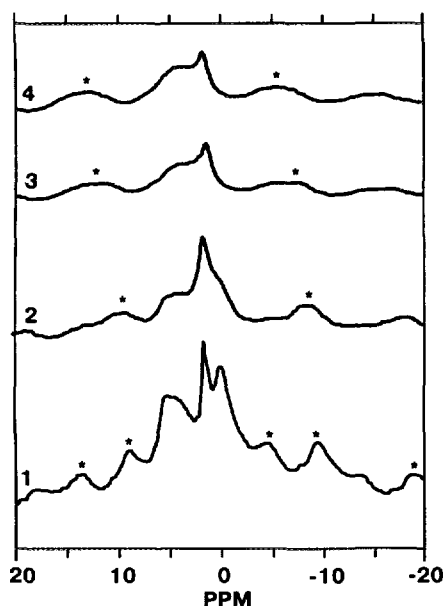


FIG. 3. ¹H-MAS NMR spectra of Al₂O₃ and catalysts after H-D exchange (evacuation at 300°C): (1) Al₂O₃ before H-D exchange; (2) Al₂O₃; (3) AlTi₂; (4) VWAlTi₂.

changes of the line shape of the ¹H-NMR signal are observed (spectra 4, 4' and 5, 5' in Fig. 2). In spectrum 4 of sample VWAlTi1 a signal of bridged Ti-OH-Ti groups at 7 ppm can still be detected. In contrast, for sample VWAlTi2 a signal from bridged Ti-OH-Ti groups cannot be seen. For VWAlTi2 the line shape also changes; the main peak is now centered at 3.4 ppm; however, the total signal intensity does not decrease within the limits of experimental accuracy. This may indicate that the interaction of vanadium and tungsten oxide species with surface Ti-OH-Ti groups takes place with the formation of V-OH and (or) W-OH groups. Note that the chemical shift of V-OH groups is close to 3 ppm (31, 32). The spectra of the samples evacuated at 500°C support the conclusions derived from the spectra of samples evacuated at 300°C. However, in this case due to the treatment at higher temperature, a decrease of the total content of OH groups occurs on the surfaces of the catalysts due to the evolution of bridged Ti-OH-Ti (or Ti-OH-Al) groups. This follows from the disappearance of shoulders at ≈7 ppm in the spectra of AlTi₂ and VWAlTi₁, and from the shift of the main peak position to high field (spectra 3, 3' and 4, 4' in Fig. 2). Interestingly, *in situ* DRIFT spectra of adsorbed ammonia (not shown) on vanadium- and tungsten-containing materials demonstrate the presence of Brønsted acidity in these multicomponent materials.

Figure 3 represents the spectra of catalysts precalcined at 300°C which were obtained after H-D exchange of OH groups, with subsequent evacuation of the samples at

300°C. They show that some of the acidic OH groups (signal at about 3.6–3.8 ppm) and of the basic OH groups ($\delta \approx -0.3$ ppm) are not exchanged and are thus located in the bulk or in closed pores of the alumina. These data also show that in our case the H-D exchange was not complete, since the peaks at 1.4 and -0.3 ppm still remain in spectrum 2 in Fig. 3, of exchanged alumina, and have increased intensities compared with those in AlTi₂ and VWAlTi₂ (spectra 3 and 4 in Fig. 3).

The decrease of the signal intensity after H-D exchange for the samples with supported TiO_x and vanadia and their similarity in intensity and chemical shifts to those for the spectra of exchanged alumina suggests that most of the new Ti-OH-Ti, Ti-OH-Al, and V-OH (and probably W-OH) groups are located on the surface and are accessible for reacting molecules.

Similar conclusions follow from the spectra of samples after H-D exchange when they were evacuated at 500°C.

2. ¹⁵N-NMR Spectra

Typical ¹⁵N-NMR spectra of N₂O adsorbed on the catalysts under study are shown in Fig. 4. The gas-phase chemical shifts for N₂O were reported to be -235.5 and -147.3 ppm for the terminal (t) and central (c) N atoms, respectively (25). As can be seen in Fig. 4, for all the samples the resonance signals of the N_t atom are shifted to lower field as compared to the gaseous state, while for

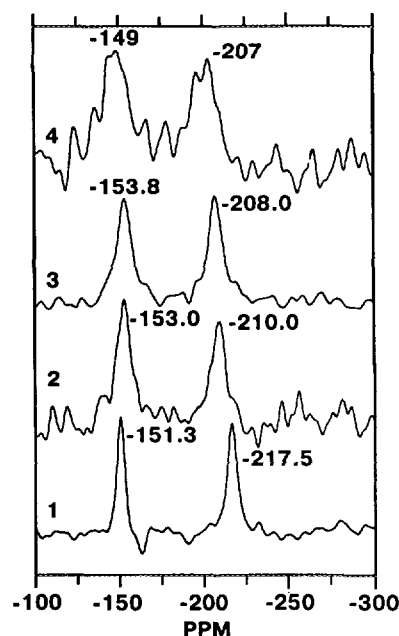


FIG. 4. ¹⁵N-NMR spectra of N₂O adsorbed on alumina, titania, and AlTi supports after evacuation at 500°C: (1) Al₂O₃, 200 μmole/g, NS = 22800; (2) AlTi₁, 140 μmole/g, NS = 6800; (3) AlTi₂, 140 μmole/g, NS = 11000; (4) TiO₂, 200 μmole/g, NS = 9000.

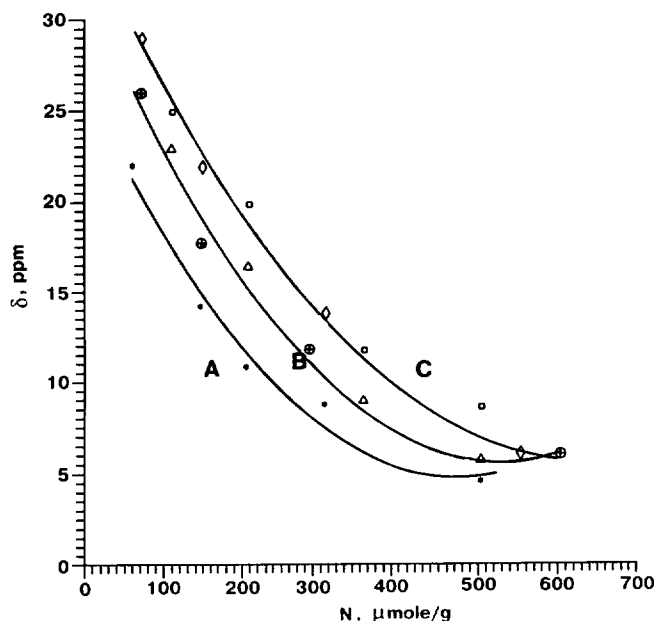


FIG. 5. Dependence of ^{15}N -NMR chemical shifts of the terminal N atom of N_2O on loading: (A, *) alumina; (B, \oplus) AlTi1; (Δ) VWAlTi1; (C, \diamond) AlTi2; (\square) VWAlTi2.

the N_c atom the observed high-field shifts are much less pronounced. This observation must be considered an indication of the interaction of N_2O via its terminal N atom with surface electron pair acceptor (Lewis acid) sites (25).

In the case of alumina these sites are known to be coordinatively unsaturated Al^{3+} cations. $\eta\text{-Al}_2\text{O}_3$ is considered to possess higher Lewis acidity than $\gamma\text{-Al}_2\text{O}_3$ due to more exposed and more easily accessible cations in anion vacancies; the concentration of strong sites per unit surface of $\eta\text{-Al}_2\text{O}_3$ interacting with adsorbed CO was reported to be three times higher than on $\gamma\text{-Al}_2\text{O}_3$ (27).

For the titania-containing samples, the observed down-field shifts of the N_i atom of N_2O are greater than those for alumina without titania additives. This may be due to a higher acid strength of the coordination sites. The value of the chemical shift increases with the increase of the titania content (spectra 2 and 3 in Fig. 4). The spectrum of N_2O adsorbed on pure anatase also shows a down-field shift of the resonance of the terminal N atom of N_2O (spectrum 4 in Fig. 4). For the VWAlTi catalysts, the ^{15}N chemical shift values do not differ significantly from those for the AlTi samples.

In order to obtain more information on the number and strength of the electron pair acceptor sites interacting with N_2O we have examined the dependences of the experimental chemical shifts for the N_i atoms (δ) on the adsorbate concentration (N) (Fig. 5). Assuming that N_2O interacts mostly with sites of one type (or different types with similar acid strength) we can evaluate the relative strength and

the number of sites from the dependence of the chemical shift δ on coverage N (Fig. 5) using an approach proposed by Borovkov *et al.* (33). Linearization of the experimental dependence of δ on N for alumina according to Borovkov *et al.* (33) in the $Nx^2/(1-x)$ vs $Nx/(1-x)$ coordinates (Fig. 6), where $x = \delta/\delta_{\text{max}}$ and δ_{max} is the chemical shift value derived from extrapolation of δ to zero loading (30 ppm from the value for physically sorbed molecules (33)), gives a value for the number of Lewis sites of $N_L = (1.9 \pm 0.4) \times 10^{17}/\text{m}^2$, the chemical shift value for the complexes of N_2O with Lewis sites L ($\text{N}_2\text{O} - L$) $\delta_c = 76 \pm 6$ ppm, and the complex formation constant $K = (3.8 \pm 1.4) \times 10^{-18} \text{ m}^2 \text{ molecule}^{-1}$. Comparing the above values with those obtained previously for $\gamma\text{-Al}_2\text{O}_3$ treated in a similar way (25), we can conclude that the concentration of sites interacting with N_2O is higher by about a factor of 2 for the present alumina, while their acid strength (the latter is assumed to be indicated by the value of the complex formation constant K) is essentially the same as for that $\gamma\text{-Al}_2\text{O}_3$ (25) and the present alumina.

It should be pointed out that although the method of linearization of the experimental data proposed by Borovkov *et al.* (33) can be used in a limited number of cases only and has some uncertainties (in particular, due to the ambiguity in the choice of the δ_{max} value), it gives reasonable values of N_L in the present case which are close to those determined from IR data of adsorbed CO (2×10^{17} molecules/ m^2).

For analyzing the Lewis acidity of the AlTi- and VWAlTi-catalysts, we have applied the same approach (Fig. 6). The calculated K , δ_c and N_L values are summarized in Table 2.

The close values of K and δ_c for the various catalysts studied demonstrate that the acid strength of the electron pair acceptor sites interacting with N_2O does not differ considerably. The higher values of the observed NMR shifts for the titania-containing samples are due to larger numbers of sites. The latter seem to be coordinatively unsaturated Ti^{4+} cations. This conclusion was confirmed also by spectra of N_2O adsorbed on anatase (spectrum 4 in Fig. 4), which also show the presence of electron pair acceptor sites.

As can be seen from Table 2, the values of K , δ_c , and N_L practically do not differ after deposition of vanadium and tungsten oxide on the AlTi supports. This fact could be an indication that the Lewis acid centers formed on supporting vanadium and tungsten oxide have an acid strength comparable to that of the strongest Lewis sites on the AlTi1 samples (coordinatively unsaturated Al^{3+} and Ti^{4+} cations) or that the sites created by deposition of V and W are larger in number but possess weaker electron accepting properties. The latter could interact with more basic test molecules, for example with ammonia, as was shown recently by IR spectroscopy (33–35). From the ex-

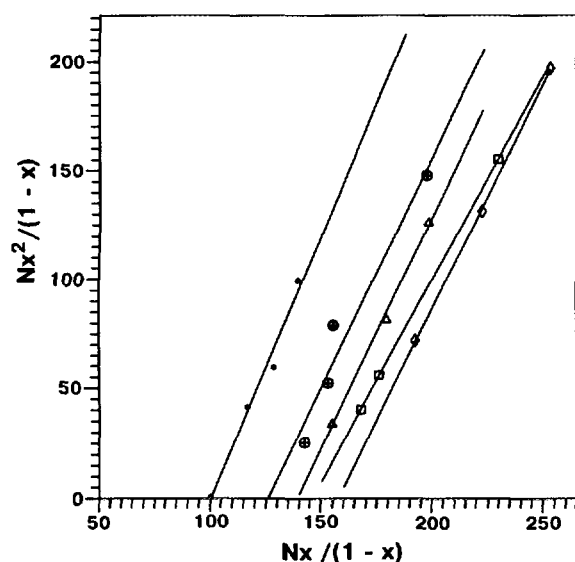


FIG. 6. ¹⁵N-NMR chemical shifts of the terminal N atom of N₂O versus coverage in the $Nx^2/(1-x)$ vs $Nx/(1-x)$ coordinates: (*) Al₂O₃; (⊕) AlTi1; (Δ) VWAiT1; (◇) AlTi2; (□) VWAiT2.

perimental data presented above it is impossible to discriminate between these two possibilities. It is interesting to note that Hilbrig *et al.* (36) detected the presence of W⁶⁺ sites on WO₃/TiO₂ catalysts by CO and NH₃ adsorption. The grafting of alumina with 3.7% TiO₂ (or 2.1×10^{18} Ti⁴⁺ ions/m²) results in an increase of N_L by 1×10^{17} /m², i.e., only a small fraction of Ti⁴⁺ cations ($\approx 1/20$) act as electron pair acceptors.

It should be noted that IR spectra of adsorbed NH₃ clearly indicated the presence of Lewis acid sites on all samples studied in this work. Moreover, thermal desorption spectra (not shown) supported the conclusions drawn from ¹⁵N-NMR spectra. In particular, thermal desorption data showed that the density of strong acid sites on AlTi-supports, and on the V and W containing catalysts was significantly higher than on the alumina support; the acid strength of the Lewis sites appeared to be comparable on AlTi and VWAiT materials.

TABLE 2

Characteristics of the Electron Accepting Properties of Al₂O₃ and of the Catalysts Supported on Al₂O₃

Sample	δ_{\max}	K [m ² × molecule ⁻¹]	δ_c [ppm]	N_L [molecules/m ²]
Al ₂ O ₃	30	$(3.8 \pm 1.4) \times 10^{-18}$	76 ± 6	$(1.9 \pm 0.4) \times 10^{17}$
AlTi1	34	$(3.4 \pm 1.2) \times 10^{-18}$	74 ± 5	$(2.7 \pm 0.5) \times 10^{17}$
VWAiT1	34	$(3.0 \pm 0.8) \times 10^{-18}$	74 ± 5	$(2.9 \pm 0.4) \times 10^{17}$
AlTi2	36	$(2.7 \pm 0.7) \times 10^{-18}$	75 ± 6	$(3.6 \pm 0.3) \times 10^{17}$
VWAiT2	36	$(3.1 \pm 0.6) \times 10^{-18}$	71 ± 5	$(3.8 \pm 0.3) \times 10^{17}$

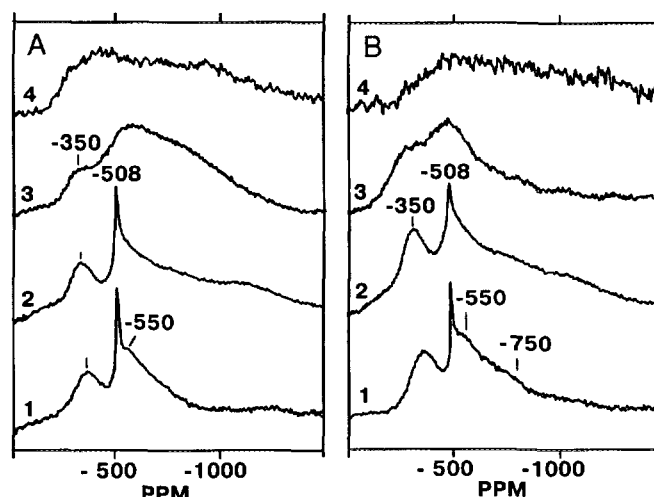


FIG. 7. ⁵¹V-NMR spectra of (V₂O₅-WO₃)/TiO₂/Al₂O₃ catalysts: (A) VWAiT1; (B) VWAiT2. (1) Magic angle spinning spectra of samples in contact with atmospheric moisture; (2) spectra of the same samples, without magic angle spinning; (3) spectra of samples evacuated at 200°C; (4) spectra of samples evacuated at 500°C.

3. ⁵¹V-NMR Spectra

⁵¹V-spectra of samples VWAiT1 and VWAiT2 are presented in Fig. 7. Four types of lines can be identified in the spectra. In the spectrum of the untreated sample (spectra 1 and 2 in Figs. 7A and 7B), a narrow line (line b) with $\delta \approx -508$ ppm belongs to the anion V₂W₄O₁₉⁴⁻ in solution in the pores of the catalysts, since its chemical shift coincides with that found for this anion in solution (37, 38). Two broader lines are also observed; line a of vanadium in tetrahedral environment with a peak at -550 ppm and line c of vanadium in distorted octahedral coordination with $\delta_{\perp} = -350$ ppm and $\delta_{\parallel} = -1270$ ppm having the parameters found earlier for V₂O₅/Al₂O₃ catalysts (39). The relative intensity of line c increases as the TiO₂ content on the alumina surface is increased (compare the spectra in Figs. 7A and 7B).

Magic angle spinning has only a small effect upon the linewidths of lines a and c, indicating that both lines most probably are inhomogeneously broadened due to a distribution of quadrupole and chemical shift parameters or due to dynamic processes in the second coordination sphere of vanadium species. The latter is known to prevent line narrowing in magic angle spinning experiments. Nevertheless, it allows one to resolve the closely spaced lines a and b, the latter having a broad shoulder near $\delta = -750$ ppm (spectra A1 and B1 in Fig. 7).

Calcination of the samples at 500°C with subsequent evacuation of adsorbed water at 200°C results in the disappearance of the narrow line at $\delta = -508$ ppm and in the broadening of the entire spectrum (spectra A3 and B3 in Fig. 7). The relative intensities of lines a, b, and c also

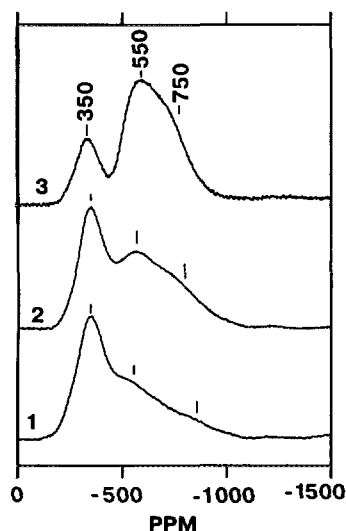


FIG. 8. ^{51}V -NMR spectra of $\text{V}_2\text{O}_5/\text{TiO}_2/\text{Al}_2\text{O}_3$ catalysts at constant V_2O_5 content (10 wt%) and different TiO_2 contents: (1) 0 wt% TiO_2 ; (2) 3 wt% TiO_2 ; (3) 10 wt% TiO_2 .

changed. Line c, which prevails in the spectrum of unevacuated samples, decreases in intensity, while the percentage contributions of lines a and b increase. For a sample of AlTi1 , containing 3.7% TiO_2 , both lines a and b are present in comparable percentages while for sample AlTi2 containing 8% TiO_2 line a prevails in the spectrum.

Evacuation of the same samples at 500°C broadens the spectrum and leads to a decrease in intensity of the spectrum (spectra A4 and B4 in Fig. 7). Lines with parameters which are very close to those observed in this work were found earlier for $\text{V}_2\text{O}_5/\gamma\text{-Al}_2\text{O}_3$ catalysts (40). Line a was attributed to VO_4 tetrahedral species loosely bound to Al_2O_3 containing OH groups in the first coordination sphere and having water molecules in the second coordination sphere. Line b was also attributed to isolated VO_4 tetrahedral species firmly bound to the surface (via two or more bonds). Line c, with an axial anisotropy of the chemical shift tensor, was observed for samples with high V_2O_5 content, and was attributed to octahedral vanadium species, having one short $\text{V}=\text{O}$ bond. However, line C for VWAlTi catalysts has a δ_{\parallel} value close to that found for the $\text{V}_2\text{O}_5/\text{TiO}_2$ system but different from that in $\text{V}_2\text{O}_5/\gamma\text{-Al}_2\text{O}_3$ catalysts. This can indicate an interaction between vanadia and TiO_2 , or it may be due to the difference in the types of alumina supports.

To verify the possibility of the influence of WO_3 on the interaction among V_2O_5 , TiO_2 , and Al_2O_3 and also to check for the possibility of formation of mixed V-W species, we have also measured the ^{51}V -NMR spectra of the system vanadia on AlTi (VAlTi) and $\text{V}_2\text{O}_5\text{-WO}_3$. The samples of the first series were prepared in a way similar to that used for preparation of VWAlTi samples, but they

did not contain WO_3 . The ^{51}V -NMR spectra of VAlTi samples with constant concentration of 10 wt% V_2O_5 and having three different concentrations of TiO_2 (0, 3, and 10 wt%) are presented in Fig. 8. It can be seen from these spectra that in nonevacuated samples the ratio between octahedral and tetrahedral V species changes in these samples in a way opposite to that in VWAlTi catalysts. Indeed, lines a and b increase in intensity while line c decreases at increasing TiO_2 content on the alumina surface. This indicates the influence of tungsten oxide on the interaction of vanadia with TiO_2 and Al_2O_3 , which was already proposed by Chen and Yang (17).

We have also found that the formation of species with V-O-W bonds is possible in the system $\text{V}_2\text{O}_5\text{-WO}_3$. This is illustrated in Fig. 9 where the ^{51}V -NMR spectra of V_2O_5 and of a mixture $\text{V}_2\text{O}_5\text{-WO}_3$ (0.5 wt% V_2O_5) after ultrahigh intensity grinding and calcination at 500°C are presented. Appearance of a peak at about -720 ppm demonstrates formation of V-O-W bonds in this sample. Inspection of the spectra of VWAlTi catalysts (Fig. 7) shows the absence of a line at $\delta = -720$ ppm, indicating that at least the same structures with V-O-W bonds are not formed in these catalysts.

CONCLUSIONS

The results presented above demonstrate that ^1H -, ^{15}N -, and ^{51}V -NMR spectra provide important information on the surface chemistry of supported vanadia on AlTi supports.

^1H -MAS NMR spectra allow one to monitor different types of OH groups of the alumina support and the formation of new OH groups bonded to TiO_x and VO_x surface species.

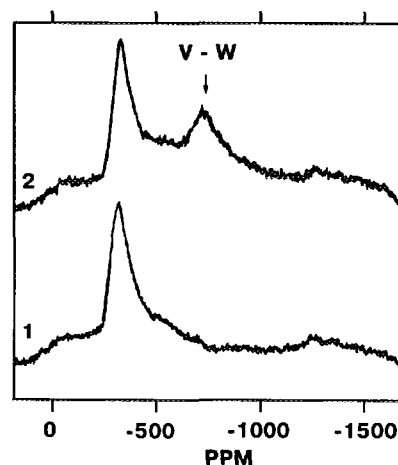


FIG. 9. ^{51}V -NMR spectra of V_2O_5 (1) and of a $\text{V}_2\text{O}_5/\text{WO}_3$ mixture (0.5 wt% V_2O_5 + 99.5 wt% WO_3) after ultrahigh intensity grinding and calcination at 500°C (2).

The increased relative intensity of the signal at $\delta = -0.3$ ppm of the alumina used as support in this study shows that, in comparison to γ -Al₂O₃, the present alumina has a higher content of basic OH groups (coordinated to one octahedral or to one tetrahedral Al atom of the Al₂O₃ surface). The latter OH groups readily interact with supported TiO_x and VO_x species. Acidic OH groups are most probably engaged in hydrogen bonds with each other and are removed from the alumina surface at 500°C. Considerable amounts of OH groups observed in ¹H-NMR spectra cannot be exchanged with D₂O and are probably located in closed pores or in the bulk of the alumina support. They are inaccessible for interaction with supported TiO_x and VO_x species. This follows from H-D exchange experiments at room temperature. Supporting TiO₂ on the alumina surface creates Ti-OH-Ti and (or) Ti-OH-Al groups. The latter can easily be removed from the support surface at 500°C, but at this temperature a considerable amount of OH groups bonded to TiO_x still remains on the surface. The structure of surface TiO_x layers is different for samples containing 3.7 and 8 wt% TiO₂. At low TiO₂ loading there is a considerable amount of H₂O in the coordination sphere of Ti after dehydroxylation at 300°C. In contrast, samples containing 8 wt% TiO₂ have no water coordinated after evacuation at 300°C, but they contain Ti-OH-Ti and probably Ti-OH-Al groups in the structure.

OH groups coordinated to Ti interact with supported vanadium and tungsten oxide species. This follows from the decrease of the line intensity at $\delta \approx 7$ ppm. Simultaneously, the formation of OH groups bonded to vanadium (and probably to tungsten) takes place, since the peak at $\delta \approx 3.4$ ppm became dominant in the spectra.

⁵¹V-NMR spectra show that the structure of surface species in VWA/Ti catalysts is different from that in VAl/Ti. This can be due to the presence of tungsten oxide in the samples under study. Although formation of V-O-W bonds has not been detected in ⁵¹V-NMR spectra, different relative intensities of lines of octahedral and tetrahedral vanadium for different TiO₂ contents show participation of tungsten oxide in the formation of the structure. The interaction of VO_x species with surface TiO_x species follows from comparison of $\delta_{||}$ with corresponding values for V₂O₅/Al₂O₃ and V₂O₅/TiO₂/Al₂O₃ catalysts. It is probable that vanadia and tungsten oxide form mixed surface species which are located on TiO_x species. Their scatter in the structure parameters results in the broadening of ⁵¹V-NMR lines and renders the detection of a line characteristic for V-O-W fragments impossible.

¹⁵N-NMR spectra of adsorbed N₂O, which permit the detection of the strongest electron pair acceptor sites, show that the alumina support used contains about twice the amount of strong Lewis sites as compared with γ -Al₂O₃. Supporting TiO₂ on alumina increases the number of

strong Lewis sites, indicating that coordinatively unsaturated Ti⁴⁺ cations on the surface of alumina act as strong electron pair acceptor sites. About 5% of supported Ti atoms create strong Lewis sites. The deposition of vanadia and tungsten oxide on AlTi does not markedly influence the number or strength of Lewis sites. This may indicate that vanadia and tungsten oxide species supported on AlTi also possess Lewis acidities similar to that of supported TiO_x species.

ACKNOWLEDGMENTS

The work done in Munich was financially supported by the Deutsche Forschungsgemeinschaft (Sonderforschungsbereich 338) and the Fonds der Chemischen Industrie, while the work done in Novosibirsk was supported by the Russian Fund for Fundamental Studies (Grant 93-03-4772). The authors thank Dr. V. F. Lyakhova (Institute of Catalysis, Novosibirsk) for preparation of the V₂O₅-WO₃ sample.

REFERENCES

1. Bond, G. C., and Tahir, S. F., *Appl. Catal.* **71**, 1 (1991).
2. Bosch, H., and Janssen, F., *Catal. Today* **2**, 369 (1988).
3. Reichmann, M. G., and Bell, A. T., *Langmuir* **3**, 111 (1987).
4. Reichmann, M. G., and Bell, A. T., *Appl. Catal.* **32**, 315 (1987).
5. Fernandez, A., Leyrer, J., Gonzalez-Elise, A. R., Munuera, G., and Knözinger, H., *J. Catal.* **112**, 489 (1988).
6. Baiker, A., Dollenmaier, P., Glinski, M., and Reller, A., *Appl. Catal.* **35**, 365 (1987).
7. Vogt, E. T. C., van Dillen, J., Geus, J., Biermann, J., and Janssen, F., "Proceedings, 9th International Congress on Catalysis, Calgary, 1988" (M. J. Phillips and M. Ternan, Eds.), Vol. 4, p. 1976. Chem. Institute of Canada, Ottawa, 1988.
8. Vogt, E. T. C., de Boer, M., van Dillen, A. J., and Geus, J., *Appl. Catal.* **40**, 255 (1988).
9. Stranick, M. A., Houalla, M., and Hercules, D. M., *J. Catal.* **106**, 362 (1987).
10. Rajadhyaksha, R. A., Hausinger, G., Zeilinger, H., Ramstätter, A., Schmelz, H., and Knözinger, H., *Appl. Catal.* **51**, 67 (1989).
11. Haukka, S., Lakomaa, E.-L., and Root, A., *J. Phys. Chem.* **97**, 5085 (1993).
12. Srinivasan, S., Datye, A.-K., Smith, M. H., and Peden, C. H. F., *J. Catal.* **145**, 565 (1994).
13. Wei, Z., Xin, Q., Guo, X., Sham, E. L., Grange, P., and Delmon, B., *Appl. Catal.* **63**, 305 (1990).
14. Centi, G., Militerno, S., Perathoner, S., Riva, A., and Brambilla, G., *J. Chem. Soc. Chem. Commun.*, 88 (1991).
15. Morikawa, S., Takahashi, K., Mogi, T., and Kurita, S., *Bull. Chem. Soc. Jpn.* **55**, 2254 (1982).
16. Tuenter, G., Leeuwen, W. F. V., and Sniepangers, L. J. M., *Ind. Eng. Chem. Prod. Res. Dev.* **25**, 633 (1986).
17. Chen, J. P., and Yang, R. T., *Appl. Catal. A Gen.* **80**, 135 (1992).
18. Zamaraev, K. I., and Mastikhin, V. I., *Colloids Surf.* **12**, 401 (1989).
19. Eckert, H., and Wachs, I. E., *J. Phys. Chem.* **93**, 6796 (1989).
20. Eckert, H., Deo, G., Wachs, I. E., and Hirt, A. M., *Colloids Surf.* **45**, 347 (1990).
21. Le Costumer, L. R., Taouk, B., Le Meur, M., Payen, E., Guelton, M., and Grimblot, J., *J. Phys. Chem.* **92**, 1230 (1988).
22. Mastikhin, V. M., Mudrakovsky, I. L., and Nosov, A. V., *Progr. NMR Spectrosc.* **23**, 211 (1991).
23. Lapina, O. B., Mastikhin, V. M., Shubin, A. A., Krasilnikov, V. N., and Zamaraev, K. I. *Progr. NMR Spectrosc.* **24**, 457 (1992).

24. Freude, D., Hunger, M., and Pfeifer, H., *Z. Phys. Chem.* **152**, 171 (1987). [Frankfurt]
25. Mastikhin, V. M., Mudrakovsky, I. L., and Filimonova, S. V., *Chem. Phys. Lett.* **149**, 175 (1988).
26. Fogar, K., and Anderson, J. R., *Appl. Catal.* **23**, 139 (1986).
27. Knözinger, H., and Ratnasamy, P., *Catal. Rev. Sci. Eng.* **17**, 31 (1978).
28. Mastikhin, V. M., Mudrakovsky, I. L., and Zamaraev, K. I., *React. Kinet. Catal. Lett.* **34**, 161 (1987).
29. Lippens, B. C., and Steggerda, J. J., in "Physical and Chemical Aspects of Adsorbents and Catalysts" (B. C. Linsen, Ed.), p. 171. Academic Press, New York, 1970.
30. Mastikhin, V. M., and Nosov, A. V., *React. Kinet. Catal. Lett.* **46**, 123 (1992).
31. Pinaeva, L. G., Lapina, O. B., Mastikhin, V. M., Nosov, A. V., and Balzhinimaev, B. S., *J. Mol. Catal.* **88**, 311 (1994).
32. Mastikhin, V. M., Nosov, A. V., Terskikh, V. V., Zamaraev, K. I., and Wachs, I. E., *J. Phys. Chem.* **98**, 13621 (1994).
33. Borovkov, V. Yu., Zaiko, A. V., Kazansky, V. B., and Hall, W. K., *J. Catal.* **75**, 219 (1982).
34. Miyata, H., Nakagawa, Y., Ono, T., and Kubokawa, Y., *Chem. Lett.*, 1141 (1983).
35. Inomata, M., Mori, K., Miyamoto, A., Vi, T., and Murakami, Y., *J. Phys. Chem.* **87**, 754 (1983).
36. Hilbrig, F., Schmelz, H., and Knözinger, H., "Proceedings, 10th International Congress on Catalysis, Budapest 1992" (L. Gucci, F. Solymosi and P. Tétényi, Eds.), p. 1351. Elsevier, Amsterdam, 1993.
37. O'Donnel, S. E., and Pope, M. T., *J. Chem. Soc. Dalton Trans.*, 2290 (1976).
38. Maximovskaya, R. I., Il'yasova, A. K., Begaliev, D. U., Takezhanova, D. F., and Akhmetova, A. K., *Izv. Akad. Nauk SSSR Ser. Khim.* **10**, 2169 (1984).
39. Lapina, O. B., Mastikhin, V. M., Simonova, L. G., and Bulgakova, Yu. O., *J. Mol. Catal.* **61**, 61 (1991).